Effect of Solvent Quality and Chain Confinement on the Kinetics of Polystyrene Bromination

Young K. Jhon, James J. Semler,† and Jan Genzer*

Department of Chemical & Biomolecular Engineering, North Carolina State University, Raleigh, North Carolina 27695-7905

Received May 25, 2008; Revised Manuscript Received July 8, 2008

ABSTRACT: We report on the kinetics of the bromination of free polystyrene (PS) chains in bulk solution and those anchored on flat solid substrates by performing the bromination reaction in different solvents, including nitrobenzene (NB), 1-chlorodecane (CD), 1-chloroundecane (CUD), and 1-chlorododecane (CDD), at various temperatures. We find that bulk bromination of PS follows the second-order kinetic in bromine and the reaction rate increases with increasing dielectric constant of the solvent (ε). In spite of $\varepsilon_{CDD} > \varepsilon_{CD}$, the bulk bromination kinetics of PS in CDD is slower than that in CD because of lower solubility of PS in CDD than in CD. In addition, we demonstrate that the reaction rates for brominating PS brushes anchored to flat solid substrates are much slower than those for brominating free PS chains in bulk solution. We attribute this behavior to steric hindrance due to PS confinement on the substrate.

1. Introduction

Over the past few decades numerous researchers reported on the formation and physicochemical properties of poly(4-bromostyrene) (PBrS) and its copolymers. These studies have been motivated by excellent flame-retarding properties[1−4] and unique phase behavior of PBrS.[5−16] A variety of synthetic methodologies for obtaining homopolymers and copolymers of bromostyrene have been described, including free radical,[17,18] cationic,[19,20] anionic,[21] and controlled radical polymerization.[22] In addition, the synthesis of random copolymers, poly(styrene-*co*-4-bromostyrene) (PBr_xS), comprising styrene and 4-bromostyrene units, has been reported that utilized bromination reaction performed on parent polystyrene (PS) coils.[23−26] The latter reaction has several advantages. First, the mole fraction of 4-bromostyrene (4-BrS) in PBr_xS can be fine-tuned to range from 0 to 100% by adjusting the reaction conditions. Second, the degree of polymerization and polydispersity index (PDI) of the resultant PBr_xS match those of the parent PS. Third, as pointed out below, by judiciously choosing the reaction conditions, one may achieve control over the degree of "blockiness" in comonomer sequence in PBr_xS.

Diverse catalysts, including $AlCl_3$, $FeCl_3$, $SnCl_4$, $SbCl_5$, $TiCl_4$, ZnO, $ZnCl_2$, and $ZnBr_2$, have been reported to increase the rate of PS bromination leading to PBr_xS.[27−35] While catalyzed bromination typically results in relatively high reaction rates, nonrecyclable catalyst waste and the purification of catalyst represent certain drawbacks for such reactions.[36−38] In their original papers, Kambour and co-workers showed that in the absence of light solvents with a moderate dipole moment, i.e., chloroform or nitrobenzene, are capable of polarizing the Br_2 molecule, thus enabling electrophilic substitution addition of bromine in the *para* position of the phenyl ring of PS without using a catalyst.[25,26] While the reaction rates have been considerably slower than those reported for catalyzed brominations, the absence of catalysts and thus ease of purification are great benefits of such "solvent-catalyzed" bromination reactions.

All bromination reactions mentioned above have been carried out under good solvent conditions. It was assumed that under such circumstances the distribution or styrene and 4-BrS units along PBr_xS was relatively random. This approximation was earlier utilized in determining the tacticity of the parent polystyrene homopolymers.[39] We have recently reported that bromination of polystyrene in short chlorinated alkane solvents produces PBr_xS that can generally be termed as "random-blocky" copolymers.[40] Specifically, we utilized 1-chlorodecane (CD), 1-chloroundecane (CUD), and 1-chlorododecane (CDD), whose theta temperatures (θ) were 6.6, 32.8, and 58.6 °C, respectively.[41−43] Depending on the solvent and the solution temperature, the PS coil can either be completely expanded ($T > \theta$), Gaussian-like ($T = \theta$), or collapsed ($T < \theta$). Because of the temperature- and solvent-dependent conformational changes of PS, bromination was expected to produce PBr_xS with different sequence distributions of 4-BrS. For example, at 32.8 °C PS was expected to adopt a swollen coil conformation in CD, Gaussian coil in CUD, and a collapsed conformation when dissolved in CDD. These assumptions were verified in experiments using electro-optical Kerr effect measurements, which confirmed that PBr_xS having the same chemical composition had more "random-blocky" character when synthesized in CDD, relative to those prepared in CD.[40]

Let us briefly compare the two extreme cases involving the bromination in good and poor solvents. In a good solvent, the parent homopolymer coil is swollen and the concentration of bromine inside the coil is approximately equal everywhere. Under such circumstances, the bromination should lead to "truly" random comonomer sequences in PBr_xS. Bromination in poor solvents is much more challenging to understand, however. First, one has to assume that there is no coagulation among PS chains during the reaction; technically, this translates to working under extremely dilute solution conditions. In our original publication[40] we provided a tentative picture of the bromination reaction in CDD. Drawing on findings obtained from small-angle neutron scattering experiments,[44] we hypothesized that as the first few styrene segments were converted into 4-BrS, the latter segments concentrated inside the collapsed PS globule because of decreased solubility of 4-BrS in CDD relative to that of PS in CDD, thus making it more compact and amendable to producing longer continuous 4-BrS sequences. These findings have recently been confirmed with computer simulations using discontinuous molecular dynamics (DMD).[45] Comparing those two extreme cases reveals that in addition to

* Corresponding author: e-mail Jan_Genzer@ncsu.edu, Ph +1-919-515-2069.
† Present address: Lexmark International Inc., Lexington, KY 40511.

10.1021/ma8011653 CCC: $40.75
Published on Web 08/21/2008

Table 1. Physicochemical Properties of Used Solvents

solvent[a]	density[b] (g/cm^3)	Θ temp for PS (°C)	dielectric constant[b]
NB	1.196	*c*	34.8
CD	0.868	6.6	2.8
CUD	0.868	32.8	3.4
CDD	0.867	58.6	4.2

[a] NB = nitrobenzene, CD = 1-chlorodecane, CUD = 1-chloroundecane, and CDD = 1-chlorododecane. [b] At 25 °C. [c] Liquid nitrobenzene is a good solvent for PS and $PBr_{1.0}S$.

the dipole moment of the solvent, the overall rate of bromination depends crucially on the accessibility of styrene segments. This notion is not that surprising. Several theoretical simulations[46−49] and experiments[50−52] have shown that physical hindrance and catalytic shape have strong influence on reaction rates and equilibrium yields in reactions involving monomers. Adding the extra complexity of steric hindrance associated with the monomer connectivity will only enhance those effects.

Here we report on the kinetics of bromination of polystyrene in solvents having different quality and different dipole moment. We show that the rate of bromination of PS depends significantly on the dielectric properties of the solvent, increasing with increasing solvent dielectric constant. Second, we demonstrate that the overall rate of bromination depends on the accessibility of styrene segments to the reacting Br_2 molecules. We illustrate this effect by (i) varying the solvent quality and (ii) performing the bromination reaction on free chains in solution as well as those that have been chemically anchored to the substrate. Our results confirm that increased chain confinement resulting from decreasing solvent quality of geometric confinement (free vs surface-anchored chains) results in slower bromination rates.

2. Experimental Section

2.1. Materials and Supplies. Monodisperse atactic polystyrene (PS) (M_w = 30 kDa, polydispersity index = 1.06) was purchased from Pressure Chemical (Pittsburgh, PA). Bromine and nitrobenzene (NB) were purchased from Aldrich Chemical Co. 1-Chlorodecane (CD), 1-chloroundecane (CUD), and 1-chlorododecane (CUD) were purchased from TCI America. Table 1 lists important physicochemical characteristics of the solvents used in this study. The polymerization initiator used in this work was (11-(2-bromo-2-methyl)propionyloxy)undecyltrichlorosilane, $Br(CH_3)_2CCOO(CH_2)_{11}SiCl_3$ (BMPUS); it was synthesized following a two-step procedure described by Matyjazsewski and co-workers.[53] *N,N,N′,N′,N″*-Pentamethyldiethylenetriamine (PMDETA), copper bromide (CuBr), copper(II) bromide ($CuBr_2$), anisole, and styrene were purchased from Aldrich Chemical Co. Silicon wafers [100] were supplied by Silicon Valley Microelectronics, Inc.; the small resistivity of the wafers (1−5 Ω·cm) facilitated infrared measurement in transmission mode (see below).

2.2. Formation of Poly(styrene-*co*-4-bromostyrene) in Bulk Solution. The reactions involving bulk solution bromination of PS were carried out in the following manner. A 1.0% (w/w) solution was placed into a controlled temperature cell, and the cell was subjected to a temperature cycle. Specifically, the cell was ramped to 70 °C (well above the θ temperature of all solvents) and maintained for 60 min. Afterward, the cell temperature was lowered to the desired temperature at a rate of 0.3 °C/min and maintained for 60 min. After completing the equilibration, a 3-fold stoichiometric excess of bromine was added to the solution under dark conditions. Bromine dissolved well in all solvents under consideration; in our analysis we thus ignored the effect of solubility of Br_2. The bromination reaction was allowed to proceed for varying times depending upon the extent of bromination desired. The resulting HBr was allowed to escape from the reaction vessel though tubing attached to the top of the reactor. The reaction was terminated by adding a few drops of 1-pentene to the reaction mixture. The samples were then purified by dissolution into toluene and subsequent precipitation into methanol. The purification step was repeated 3−5 times in order to eliminate any residual reactants and/or solvent. The polymer was then dried at 60 °C under 30 in. of vacuum in order to remove the final traces of methanol.

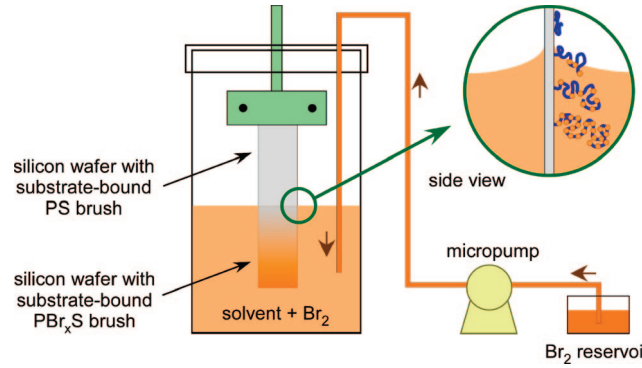

Figure 1. Schematic of the apparatus used to prepare surface-bound PBr_xS brushes with variable degree of bromination.

Table 2. Conditions for Preparing Surface-Anchored PBr_xS Brushes

sample ID	solvent[a]	solvent amount (mL)	Br_2 amount (g)	dry PS brush thickness (nm)
SA-NB1	NB	100	3.2	85.0
SA-NB2	NB	100	9.6	95.0
SA-NB3	NB	100	20.8	101.2
SA-CD1	CD	100	6.8	67.9
SA-CD2	CD	100	9.8	103.9
SA-CD3	CD	100	22.1	200.0
SA-CDD1	CDD	100	6.9	122.0
SA-CDD2	CDD	100	9.8	103.8
SA-CDD3	CDD	100	28.2	200.0

[a] NB = nitrobenzene, CD = 1-chlorodecane, and CDD = 1-chlorododecane.

2.3. Formation of Polystyrene Brushes on a Flat Silicon Substrate. Silicon wafers were cut into 1 × 7 cm^2 pieces and subjected to ultraviolet/ozone treatment for 15 min in order to generate a large number of surface-bound hydroxyl groups. The surfaces of the silicon wafers were functionalized with the BMPUS polymerization initiator using the method described previously[54] and were subsequently rinsed with toluene in order to remove any physically absorbed BMPUS molecules. Styrene monomer was filtered thorough alumina filled column before polymerization.[55] Polystyrene brushes were grown via a "grafting from" method from the substrate-bound BMPUS centers by following the atom transfer radical polymerization (ATRP) mechanism.[53,56,57] Specifically, PMDETA (0.19 mg, 1.116 mmol), CuBr (0.12 g, 0.837 mmol), $CuBr_2$ (1.5 mg, 6.715 μmol), anisole (34.8 g, 0.322 mol), and styrene (31.8 g, 0.305 mol), were charged to a 100 mL Schlenk flask equipped with a magnetic stirrer bar, sealed with a rubber septum, and degassed by sonicating and purging with nitrogen for 1 h. The polymerization of styrene was allowed to proceed at 90 °C for 24 h, after which the silicon wafer was removed and sonicated in toluene.[58] The molecular weight of PS brushes (M_n) is linearly related to the dry thickness of PS brushes on silicon wafer (h): $h = \sigma M_n/(N_A\rho)$, where σ is the grafting density (estimated to be ≈0.45 nm^2, see below), N_A is the Avogadro's number, and ρ is the density of polystyrene (1.05 g/cm^3).[59] After polymerization, the resulting PS brushes were subjected to bromination in order to create surface-anchored PBr_xS brushes, as described next.

2.4. Formation of Poly(styrene-*co*-bromostyrene) Brushes on a Flat Silicon Substrate. We utilized a gradient sample geometry in order to monitor the bromination kinetics of surface-anchored PS on a single specimen. As shown in Figure 1, a silicon wafer covered with PS brushes was placed vertically into a custom-designed reaction chamber that was kept at 25 °C. A syringe pump was used to deliver Br_2 solution of a given concentration (specified in Table 2 to the bottom of the reaction chamber at a fixed flow rate (0.4 mL/h). These experiments were executed in the absence

of light to prevent any photolysis of bromine. After bromination, the surface of the silicon wafer was washed with 1-pentene and sonicated in toluene in order to remove any unreacted Br_2 and impurities. PBr_xS brush samples were prepared by carrying out the bromination reaction in different solvents, including NB, CD, and CDD.

2.5. Ellipsometry. The thickness of polystyrene brushes was measured at various points on the silicon specimen (in a grid of 5.0 mm for longer direction) using a variable angle spectroscopic ellipsometry (VASE; J.A. Woollam, Inc.). The thickness was evaluated from the experimentally measured ellipsometric angles Ψ and Δ collected at 400−1100 nm and 70° (angle between the direction of the beam and the sample normal) using the J.A. Woollam commercial software (WVASE32). The following refractive indices were used for various material: 1.45 for BMPUS and 1.591 for polystyrene[59] at 633 nm. Table 2 lists mean thickness values collected from each sample (error less than 10%).

2.6. Fourier Transform Infrared (FT-IR) Spectroscopy. All IR spectra were acquired on a Nicolet 6700 FT-IR spectrometer with OMNIC software version 6.0 (Thermo Fisher Scientific, Inc.). The spectra of bulk PBr_xS were recorded on a thin sample film prepared on a KBr crystal. The spectra of PBr_xS brush samples on silicon wafer were obtained directly in the transmission mode. In each measurement, 2048 scans were collected with resolution 4 cm^{-1} for each measurement.

2.7. Nuclear Magnetic Resonance (NMR). Pulsed field NMR experiments were performed on a Bruker AVANCE 500 MHz spectrometer equipped with an Oxford Narrow Bore Magnet, SGI INDY host workstation, and XWINNMR software version 2.5. The NMR probe was tuned to the ^{13}C frequency, which is at 125.75 MHz for the 500 MHz spectrometer. All quantitative measurements were carried out using a single frequency 5 mm carbon ^{13}C dedicated probe (Ge NMR adopted for Bruker shims). NMR experiments revealed that the bromination occurred exclusively in the *para* position of the phenyl ring of PS and confirmed the results of the elemental analysis concerning the molar content of 4-BrS in the sample.[40]

2.8. Elemental Analysis (EA). The concentration of bromine in each PBr_xS sample was established by elemental analysis (Atlantic Microlabs, Norcross, GA).

2.9. Other Characterization Techniques. Size exclusion chromatography experiments on polymers before and after bromination established that bromination increased the molecular weight of the parent PS but did not affect the distribution of the molecular weight (i.e., no chain scission or branching took place). Differential scanning calorimetry established the presence of a single glass transition temperature revealing that, on average, all PS chains underwent bromination.[40] The same conclusions were reached from independent experiments using interaction chromatography, which revealed that no unbrominated PS was present in the solution.[61]

3. Results and Discussion

3.1. IR Spectra Analysis. We utilized FT-IR spectroscopy to determine the mole fraction of 4-BrS in PBr_xS, in addition to using ^{13}C NMR and EA. Application of FT-IR was motivated by our needs to measure the content of 4-BrS in PBr_xS brushes; neither ^{13}C NMR nor IR analysis could be applied there because of our inability to produce a sufficient amount of material. Because IR provides concentration information on a relative basis, we used bulk-synthesized PBr_xS as standards.[62] The monosubstituted phenyl ring exhibits a characteristic absorption peak at ≈698 cm^{-1}. 4-BrS is characterized by the 1,4-disubstituted phenyl ring with its absorption peak at ≈821 cm^{-1} and the bromine compound ring with absorption peaks at ≈1010 and ≈1408 cm^{-1}.[63] The methylene $-CH_2-$ stretching vibration at ≈2925 cm^{-1} served as a reference signal as the $-CH_2-$ groups were unaffected by the bromination reaction. In Figure 2 we plot IR spectra for PS for several selected bulk PBr_xS samples with various degrees of bromination ranging from 0% (pure PS) to 100% ($PBr_{1.0}S$). In Figure 3 we plot the normalized

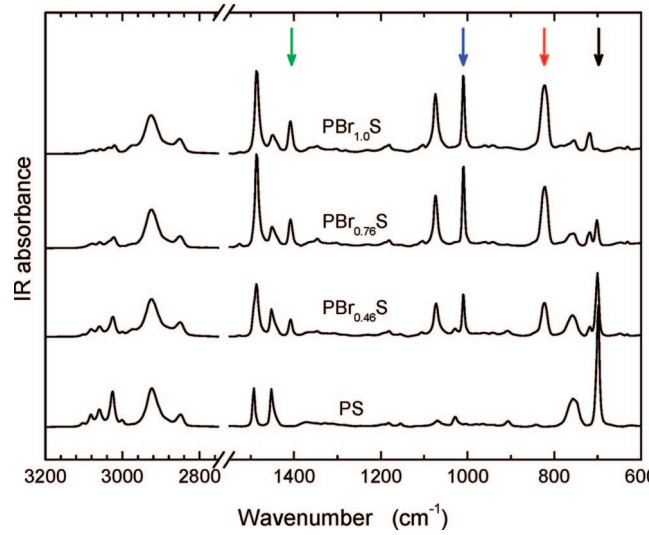

Figure 2. Infrared absorption spectra for PS and PBr_xS, where x denotes the mole fraction of 4-bromostyrene (4-BrS). In the figure we mark the following characteristic peaks: monosubstituted phenyl ring (≈698 cm^{-1}), 1,4-substituted phenyl ring with in PBr_xS (≈821 cm^{-1}), and bromine-containing phenyl ring (≈1010 and ≈1408 cm^{-1}). The methylene $-CH_2-$ stretching vibration at ≈2925 cm^{-1} serves as a reference for signal as the $-CH_2-$ groups are unaffected by the bromination reaction.

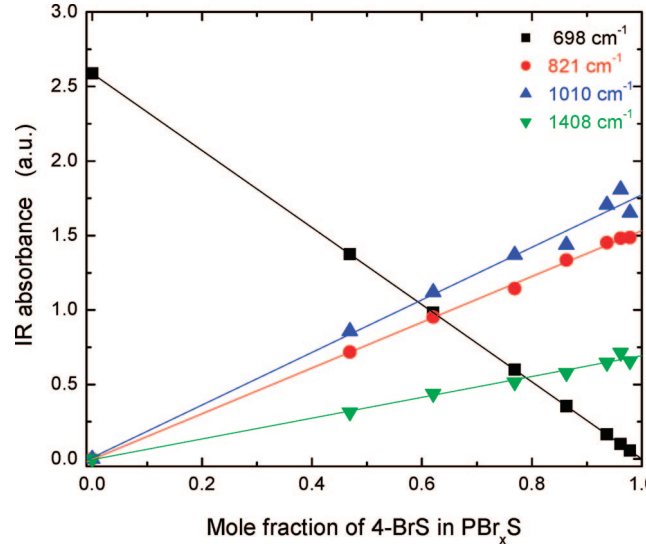

Figure 3. Intensities of IR absorbances for 4 characteristic peaks indicated in Figure 2 (cf. legend to Figure 2) as a function of the mole fractions of 4-BrS in PBr_xS. The lines are best fits to the data. With increasing degree of bromination, the absorbance intensity corresponding to pure PS (≈698 cm^{-1}) decreases while those referring to the presence of the Br-phenyl signal (≈821, ≈1010, and ≈1408 cm^{-1}) increase.

IR intensities for the aforementioned characteristic wavenumbers as a function of the mole fraction of 4-BrS, which was determined via elemental analysis. As apparent from the plot, increasing the degree of bromination leads to a decrease in the ≈698 cm^{-1} frequency intensity, indicating decreasing number of unbrominated styrene units, and an increased intensity at the wavenumbers, indicating the presence of 4-BrS. We use these correlations to quantify the degree of bromination in PBr_xS brushes on solid substrates.

3.2. Bromination of PS Coils in Different Solvents and at Different Temperatures. We monitored the rate of bromination in four solvents: NB, CD, CUD, and CDD at temperatures

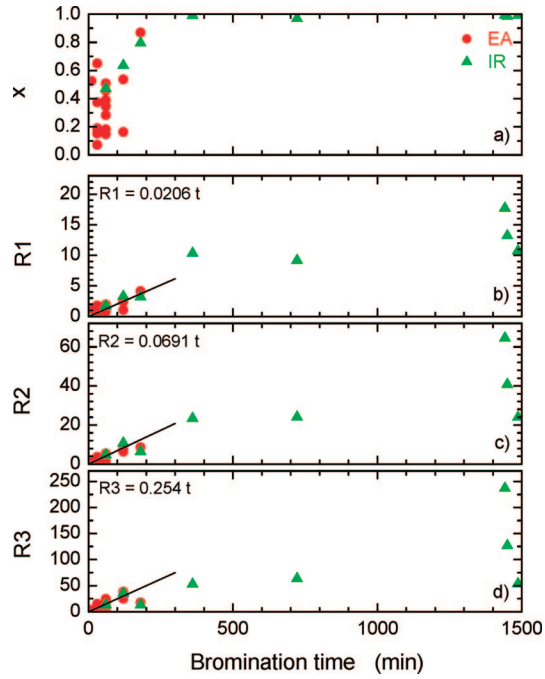

Figure 4. (a) Degree of bromination (x) determined by elemental analysis (EA, circles) and infrared spectroscopy (IR, triangles), and the corresponding values of (b) R1, (c) R2, and (d) R3, calculated using eqs 4−6, as a function of bromination time for bromination of PS (30 kDa) in nitrobenzene (NB) at 25 °C. The lines are best fits to the data for $x < 1$. The equations corresponding to the best fits are given in the respective figures.

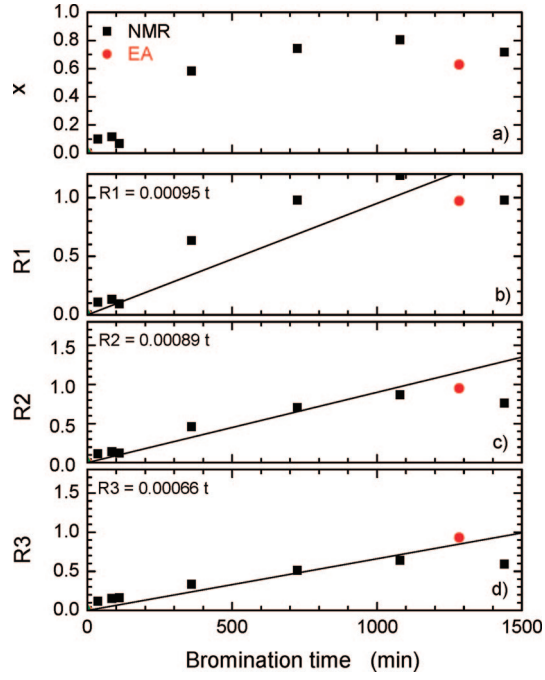

Figure 5. (a) Degree of bromination (x) determined by nuclear magnetic resonance (NMR, squares) and elemental analysis (EA, circles) and the corresponding values of (b) R1, (c) R2, and (d) R3, calculated using eqs 4−6, as a function of bromination time for bromination of PS (30 kDa) in 1-chlorodecane (CD) at 32 °C. The lines are best fits to the data for $x < 1$. The equations corresponding to the best fits are given in the respective figures.

ranging from 20 to 60 °C. NB is a good solvent for PS and PBr_xS at all reaction temperatures. As already mentioned, the θ temperatures of CD, CUD, and CDD are 6.6, 32.8, and 58.6 °C, respectively. In parts a of Figures 4−6 we plot the degree

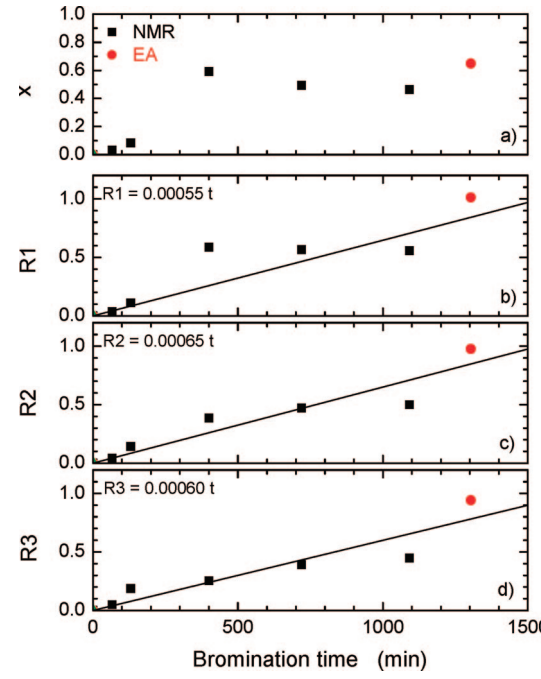

Figure 6. (a) Degree of bromination (x) determined by nuclear magnetic resonance (NMR, squares) and elemental analysis (EA, circles) and the corresponding values of (b) R1, (c) R2, and (d) R3, calculated using eqs 4−6, as a function of bromination time for bromination of PS (30 kDa) in 1-chlorododecane (CDD) at 32 °C. The lines are best fits to the data for $x < 1$. The equations corresponding to the best fits are given in the respective figures.

of bromination (i.e., the content of 4-BrS in PBr_xS), determined by FT-IR (triangles), NMR (squares), and EA (circles), as a function of the bromination time. The data shown correspond to the bromination in NB at 25 °C (cf. Figure 4), CD at 32 °C (cf. Figure 5), and CDD at 32 °C (cf. Figure 6). From the data it becomes apparent that bromination of PS in NB (cf. Figure 4) is the fastest among the three reactions, reaching a 100% degree of bromination in less than 400 min under the conditions of the experiment. This finding is not that surprising if one considers that the reaction rate depends on the dielectric constant of the solvent, ε (bromination reaction rate increasing with increasing ε), and solvent quality. Recall that NB is a good solvent for both PS and PBr_xS and possesses the highest dielectric constant among all solvents considered here. Even after more than 1000 min, bromination of PS in CD and CDD does not reach the full level of bromination; instead, the maximum levels of bromination in CD and CDD are ≈80 and ≈60%, respectively. Considering that CD and CDD are good and poor solvents, respectively, for PS under the conditions of the experiments, these results indicate that the conformation of PS in the solvent determines the maximum level of bromination due to accessibility of styrene segments during the "coloring" reaction.[64,65]

We now turn to a more quantitative analysis of the bromination kinetics. In the past, several research groups studied the bromination of styrene (or styrene-like monomers) as well as polystyrene under various conditions.[27−30,32−34,66−72] For instance, Robertson et al. reported that the bromination of mesitylene in acetic acid follows a second-order kinetics at low bromine concentrations (10^{-2}−10^{-3} M).[73−75] Andrews[76,77] and Wright groups[31] argued that bromination substitution follows a

Scheme 1. Overall Reaction Scheme of Depicting the Bromination of Polystyrene with Bromine

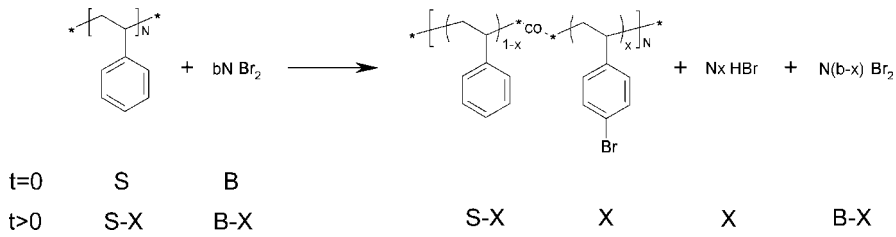

combined first-order (in bromine) and second-order (in bromine) reaction kinetics.

$$R = -\frac{d[Br_2]}{dt} = k_1[ArH][Br_2] + k_2[ArH][Br_2]^2 \quad (1)$$

Specifically, Andrews et al. studied the kinetics of bromination of mesitylene in acetic acid, and Wright et al. investigated the kinetics of bromination of six substituted styrenes (3-fluoro-, 3-chloro-, 3-bromo-, 3,4-dichloro-, 3-nitro, and 4-nitro-) in anhydrous acetic acid at temperatures between 17 and 45 °C. From their data it appears that the second-order kinetics in bromine is most dominant because $k_1/k_2 \ll 1$.[31,76,77] Jungers et al. described the bromine substitution on the *para* position of toluenes and xylenes using a third-order kinetics in bromine.[66,67,78,79] Camps et al. showed that bromination of polystyrene in the presence of Lewis acid catalysts, i.e., $SnCl_4$, $SbCl_5$, and $TiCl_4$, is of fourth order (third order in bromine).[27]

In our work, we examine three possible reaction orders. On the basis of the reaction scheme shown in Scheme 1, we write down a general kinetic balance for the bromination reaction as

$$-\frac{d(S-X)}{dt} = \frac{dX}{dt} = k_{exp}(S-X)(B-X)^Z \quad (2)$$

In eq 2, S and B represent the molar concentrations of styrene and bromine, respectively, X is the molar concentration of 4-bromostyrene, k_{exp} is the rate constant for bromination, and Z is the reaction order. Equation 2 has a general solution given by

$$\int_0^X \left(\frac{dX}{(S-X)(B-X)^Z}\right) = \int_0^t k_{exp}\, dt \quad (3)$$

The solutions to eq 3 for $Z = 1$, 2, and 3 can be obtained after some algebra. Those read as follows:
For $Z = 1$

$$R1 = k_{exp}t = \frac{1}{B-S}\ln\left(\frac{S}{B}\frac{B-X}{S-X}\right) \quad (4)$$

for $Z = 2$

$$R2 = k_{exp}t = \frac{1}{(B-S)^2}\ln\left(\frac{S}{B}\frac{B-X}{S-X}\right) - \frac{1}{B-S}\frac{X}{B(B-X)} \quad (5)$$

and for $Z = 3$

$$R3 = k_{exp}t = \frac{1}{(B-S)^3}\ln\left(\frac{S}{B}\frac{B-X}{S-X}\right) - \frac{1}{(B-S)^2}\frac{X}{B(B-X)} - \frac{1}{2(B-S)}\frac{2BX-X^2}{B^2(B-X)^2} \quad (6)$$

R1, R2, and R3 are represented by the second-order (first order in bromine), third-order (second order in bromine), and fourth-order (third order in bromine) reaction rates, respectively. We used the experimentally measured values of x for four different solvents and bromination temperatures ranging from 20 to 60 °C to determine the rate constants, k_{exp}, using eqs 4−6. The rate constants, k_{exp}, were extracted from the best fits to the slopes. Typical plots pertaining to the bromination of PS in NB, CD, and CDD are shown in parts b−d of Figures 4−6. In Figure 7 we plot k_{exp} (in a semilogarithmic plot) as a function of the inverse temperature for PS brominated in NB (diamonds), CD (squares), CUD (circles), and CDD (triangles) for the third-order bromination reaction (second order in bromine). These data can be used to determine the activation energy for bromination (E_A) from

$$k_{exp} = Ae^{-E_A/RT} \quad (7)$$

In eq 7, A is a (frequency) prefactor, R is the universal gas constant (8.314 J/(mol/K)), and T is the absolute temperature. The E_A value can be readily extracted from the slope in a plot of $\ln(k_{exp})$ against $1/T$ (i.e., slope $= -E_A/R$). These activation energies determined for the first (squares), second (circles), and third (triangles) reaction in bromine in NB, CD, CUD, and CDD are shown in Figure 8a.

It is challenging to make conclusions about the actual rate of bromination from the fits, whose representative examples are shown in parts b−d in Figures 4−6. However, examining the results in Figure 8a does provide evidence that the reaction is first order in styrene and second order in bromine. First, one can rule out the first-order reaction in bromine because E_A for CD should not be higher than that in CDD; brominating PS in CD is easier than that in CDD due to conformational constraints associated with the PS chain. Also, the fits to the experimental data using the first-order reaction in bromine are consistently worse than those obtained using the second- and third-order reaction mechanisms (cf. Figures 5 and 6). Second, considering that the rate of bromination increases with increasing the dielectric constant of the solvent, the results obtained for the third-order reaction in bromine do not seem feasible as $\varepsilon_{NB} \gg \varepsilon_{CD}$. In the presence of solvent with a high dielectric constant, two bromine molecules separate to tribromide anion and

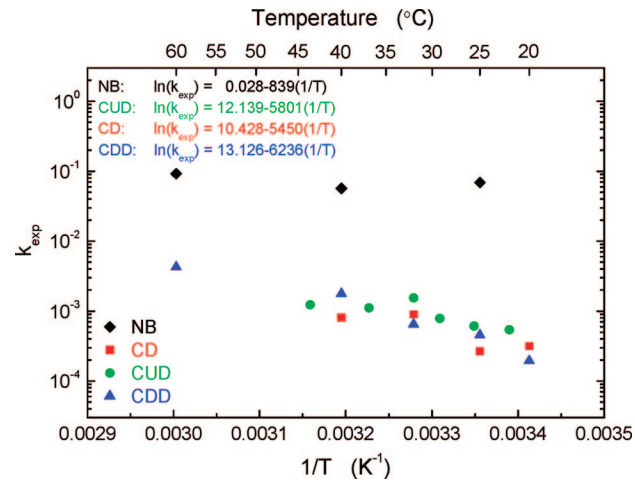

Figure 7. Bromination rate constants corresponding to the third-order bromination reaction of PS (second order in bromine) in nitrobenzene (NB, diamonds), 1-chlorodecane (CD, squares), 1-chloroundecane (CUD, circles), and 1-chlorododecane (CDD, triangles) as a function of reciprocal temperature for temperature ranging from 20 to 60 °C.

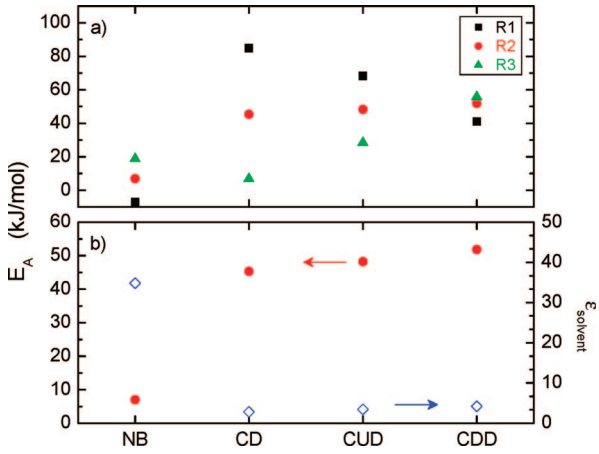

Figure 8. (a) Activation energies (closed symbols, left ordinate) obtained from first (squares), second (circles), and third (triangles) order (in bromine) reaction analysis for bromination of PS (30 kDa) in nitrobenzene (NB), 1-chlorodecane (CD), 1-chloroundecane (CUD), and 1-chlorododecane (CDD). (b) (left ordinate) Activation energies the second-order (in bromine) reaction analysis for bromination of PS (30 kDa) and (right ordinate) dielectric constant (open diamonds, right ordinate) at 25 °C in NB, CD, CUD, and CDD.

bromide cation. The bromination reaction then follows electrophilic aromatic substitution by a linear Br_3^-,[37,80,81] as shown in Scheme 2. This chemical route is in accord with our ^{13}C NMR analysis, which confirmed that the substitution of hydrogen for bromine occurred only in the *para* position of the phenyl ring of PS.[40]

In Figure 8b we plot the activation energy for bromination assuming the second order in bromine (left ordinate, circles) and the dielectric constant of the solvent (right ordinate, open diamonds) for NB, CD, CUD, and CDD. The data indicate that there is inverse relationship between E_A and ε, as expected. While ε for NB is 10−20 times higher than that in CD, CUD, and CDD for temperatures ranging from 20 to 60 °C, E_A in NB is ≈10 times lower than those in CD, CUD, and CDD. Because of the higher ε, tribromide in NB may more strongly attack the aromatic rings in PS with highly oriented electrophiles compared with tribromides in CD, CUD, and CDD. Activation of bromide substituents stabilizes the intermediate formed during the substitution by donating electrons into the phenyl ring by resonance and stronger inductive effects (cf. Scheme 2). The data in Figure 8 reveal another interesting fact. Namely, while ε for CDD is higher than that in CD (cf. Table 1), the value of E_A in CDD is higher than that in CD. One may reconcile this observation by invoking the effect of solvent quality, which affects the conformation of PS, as discussed earlier. To this end, substitution of the hydrogen atom in the *para* position of the phenyl ring in PS should be easier when performed in CD, relative to CDD, because PS adopts "open chain" conformations in CD relative to CDD. Because of the steric hindrance associated with collapsed conformations in CDD, the accessibility of unsubstituted styrene units in PS to bromine atoms is limited. It thus appears that the rate of bromination depends not only on the chemical reaction environment but also on the degree of the physical accessibility of bromine to phenyl ring in PS. We provide further evidence about this in the next section where we discuss the bromination of polystyrene chains anchored chemically to flat solid substrates.

3.3. Bromination of Surface-Anchored PS Brushes in Different Solvents. The two-step method leading to the formation of surface-tethered PBr_xS, which facilitated monitoring the bromination kinetics in surface-confined PS chains on a single specimen, has been described earlier in the Experimental Section. Recall that in the first step we prepared PS brushes anchored to a flat silica substrate via surface-initiated ATRP of styrene. In the following step, we have carried out the bromination reaction using the setup illustrated in Figure 1. Specifically, the silicon wafer decorated with surface-bound PS brushes was placed vertically into a reaction chamber, and Br_2 solution was delivered via a syringe pump to the bottom of the reaction chamber at a fixed flow rate. The bromination of PS brushes was carried out in NB, CD, and CDD at 25 °C. The degree of bromination of surface-anchored PBr_xS brushes was monitored via FT-IR. In order to convert the IR intensities into the mole fraction of 4-BrS, we used the calibration plot relating the IR intensities of selected frequencies to the mole fraction of 4-BrS in bulk-synthesized PBr_xS determined by EA (cf. Figure 2).

In order to calculate the amount of styrene present in PS brushes, we had to make an assumption about the overall grafting density of PS brushes on the substrate (σ_{PS}). On the basis of our previous work,[82,83] we estimate $\sigma_{PS} \approx 0.45$ chains/nm^2. Using this approximation, we can relate the dry thickness of PS brushes (h_{PS}) to the molecular weight (M_{PS}) via

$$M_{PS} = 1200 h_{PS}$$

where h is in nanometers and M_{PS} is in daltons. Considering that the width of the substrate is w (recall, we typically used $w \approx 1$ cm) and the immersion depth in the bromination solution is y, the number of chains immersed in solution is

$$c_{PS} = \sigma_{PS} w y \tag{8}$$

and the total PS mass is

$$m_{PS} = \sigma_{PS} w y \frac{M_{PS}}{N_A} \tag{9}$$

where N_A is Avogadro's number. At any given time, the height of the bromination solution in the reactor is the same as the immersion depth of the sample, y. Considering the total volume of the liquid to be given by $\pi d^2 y/4$, where d is the inner diameter of the reactor vessel, the molar concentration of styrene units, S (in mol/L), can be estimated from

$$S = \frac{4\sigma w M_{PS}}{\pi d^2 N_A M_S} \times 10^{15} \tag{10}$$

In eq 10, M_S is the molecular weight of styrene (= 104.15 Da).

In Figures 9a−11a we plot the concentration of 4-BrS units in surface-tethered PBr_xS brushes as a function of bromination time. As expected, in each solvent the degree of bromination increases with increasing the content of bromine in the solution. Note that the molar concentration of Br_2 in the bromination solution is much higher relative to the bulk bromination described and discussed earlier (n_{Br}/n_S = 1.3-7.0 for bulk bromination and 1.3×10^7−7.0×10^7 for surface bromination; n_{Br} and n_S represent the molar concentrations of bromine and styrene, respectively). In order to compare the results for PBr_xS brushes prepared in three different solvents more quantitatively, in Figure 12 we replot the mole fraction of 4-BrS in PBr_xS brushes as a function of bromination time for systems having approximately the same thickness of PS brush and the same concentration of Br_2 in solution. Comparison of the data in Figure 12 reveals that bromination in NB, a good solvent for PS and PBr_xS, is the fastest among the three solvents. In addition, bromination of PS brushes in CD was only slightly faster than that performed in CDD.

We used eqs 4−6 in order to calculate the rate constants R1−R3 in NB, CD, and CDD. The results are plotted in parts b−d of Figures 9−11. In our analysis we omit effects associated with differences in the PS brush thickness because the amount of bromine during the bromination reaction is much higher than

Scheme 2. Scheme of Bromination Mechanism of Polystyrene with Bromine

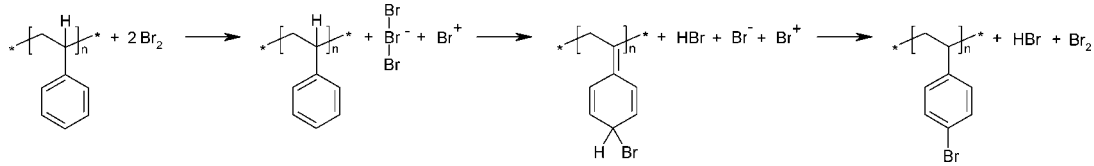

the concentration of styrene units in the sample. Because of the large scatter in data, it is not easy to make quantitative conclusion about the reaction order. However, we can rule out the possibility of the third-order reaction in bromine because the data collected from three individual bromine concentrations (parts d of Figures 9−11) do not match for either solvent. On the basis of the match among the three data sets for each solvent, we make the following conclusions. For NB, the reaction appears to follow the first-order kinetics in bromine. The reaction rate, based on the fits, appears to be more than 5.5 times slower relative to bulk bromination. Bromination of PS brushes in CD and CDD appears to be either first or second order (or the combination of first and second order) in bromine; the reaction rates are reduced about twice relative to the bromination in bulk for both solvents. While more experiments would have to be carried at various temperatures for each solvent in order to confirm the reaction order and extract the E_A values, it is clear that the bromination kinetics of PS brushes is much slower relative to that of free PS chains. We attribute this behavior to the steric hindrance due to confining PS chains at the interface.

4. Conclusions

We conclude by summarizing our findings and making a few remarks. In this paper we have reported on the brominations of PS chains in bulk and surface-anchored PS brushes in four different solvents and various temperatures. We find that (i) the bulk bromination of PS follows the second-order kinetics in bromine and (ii) the reaction rate increases with increasing dielectric constant of the solvent. We also find that the bromination kinetics depends on the solvent quality. To this end, experiments in CD and CDD revealed that bromination in CDD is slower than that in CD in spite of the fact that the dielectric constant of CDD is higher than that of CD. We explain this observation by considering that the solubility of PS in CDD is lower than that in CD. In addition to bromination of PS chains in bulk, we have also studied the formation of PBr_xS brushes on flat solid substrates by brominating PS chains that were previously formed by surface-initiated polymerization of styrene. Using a combinatorial setup, we monitored the entire bromination kinetic in a given solvent at 25 °C on a single sample. Analysis of the kinetic data from PBr_xS brushes reveals that the reaction order for bromination appears to be of first order in bromine for NB and either first or second order (or the combination of first and second order) in bromine for CD and CDD. We cautioned that a more detailed set of experiments has to be carried out at different temperatures in order to confirm these findings and in order to extract the values of E_A. We have, however, conclusively shown that the reaction rates for brominating PS brushes are much slower than those for brominating free PS chains in solution. We attribute this behavior to steric hindrance due to PS confinement on the substrate.

We are aware of the various complexities involved in postpolymerization reactions on surface-confined macromolecules. While not explicitly stated, in all our analysis we

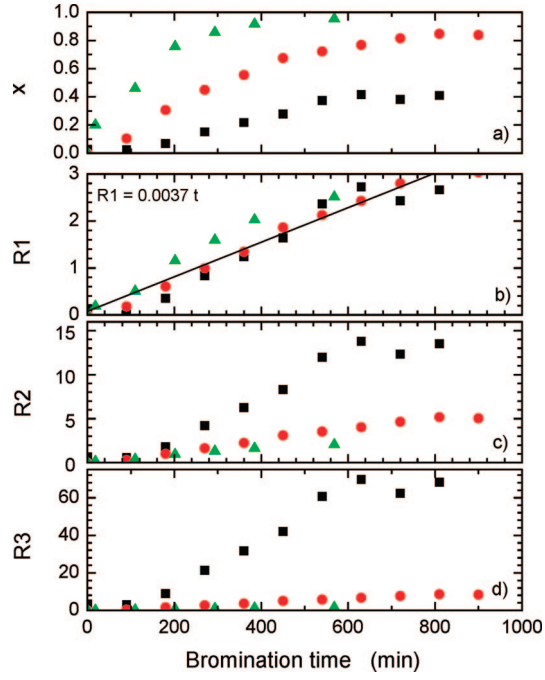

Figure 9. (a) Degree of bromination (x) determined by infrared spectroscopy and the corresponding values of (b) R1, (c) R2, and (d) R3, calculated using eqs 4−6, as a function of bromination time for bromination of PS brushes in nitrobenzene (NB) at 25 °C. The symbols denote various experimental conditions corresponding to samples SA-NB1 (black squares), SA-NB2 (red circles), and SA-NB3 (green triangles). See Table 2 for sample description.

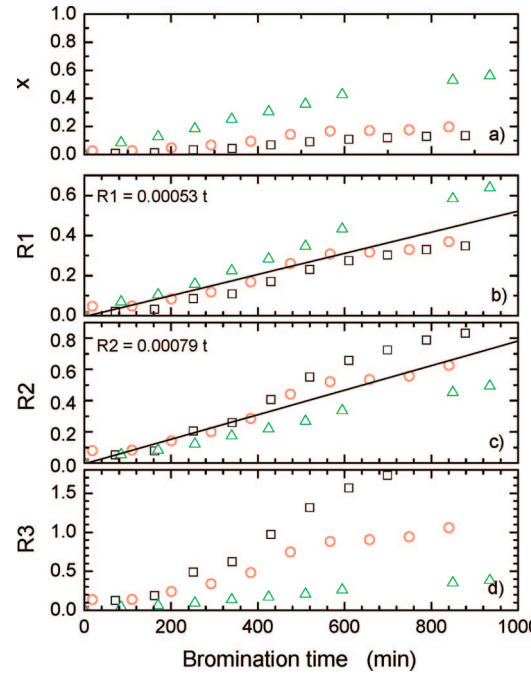

Figure 10. (a) Degree of bromination (x) determined by infrared spectroscopy and the corresponding values of (b) R1, (c) R2, and (d) R3, calculated using eqs 4−6, as a function of bromination time for bromination of PS brushes in 1-chlorodecane (CD) at 25 °C. The symbols denote various experimental conditions corresponding to samples SA-CD1 (black squares), SA-CD2 (red circles), and SA-CD3 (green triangles). See Table 2 for sample description.

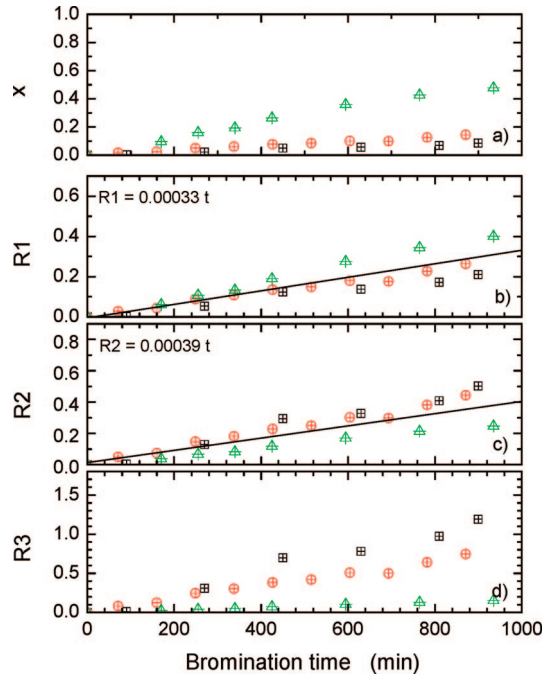

Figure 11. (a) Degree of bromination (x) determined by infrared spectroscopy and the corresponding values of (b) R1, (c) R2, and (d) R3, calculated using eqs 4−6, as a function of bromination time for bromination of PS brushes in 1-chlorododecane (CDD) at 25 °C. The symbols denote various experimental conditions corresponding to samples SA-CDD1 (black squares), SA-CDD2 (red circles), and SA-CDD3 (green triangles). See Table 2 for sample description.

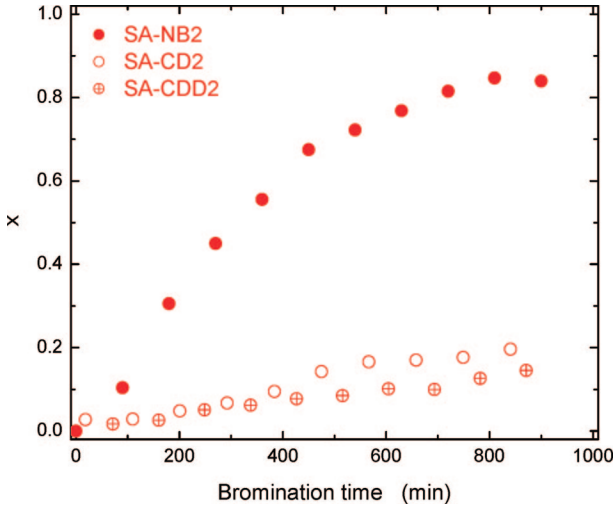

Figure 12. Degree of bromination (x) as a function of bromination time for bromination of PS brushes in nitrobenzene (NB), 1-chlorodecane (CD), and 1-chlorododecane (CDD) at 25 °C. The amount of bromine, the amount of solvent, and dry thickness of the parent PS brush are approximately the same in all samples. See Table 2 for sample description.

assumed that Br_2 can penetrate PS brushes completely. Recent computer simulations have revealed that, depending on the chain grafting density, chemical reactions performed on surface-anchored polymers may lead to the formation of copolymers with various comonomer sequences[84] While "coloring" sparsely spaced brushes on flat substrates consistently produces random copolymers, increasing the density of the brush leads to the formation of surface-grafted copolymers, whose bottom block comprises the original parent polymer and the top block is made of a random copolymer consisting of the "uncolored" and "colored" moieties. Preliminary experiments using neutron reflectivity on samples brominated in NB, CD, and CDD confirm our assumptions about equal distribution of 4-BrS along the PBr_xS brushes—at least for the grafting densities of PS chains considered in this paper ($\sigma_{PS} \approx 0.45$ chains/nm^2).[85] In order to gain complete understanding of the effect of chain confinement, it would be important to carry out bromination of PS brushes in different solvents at various values of σ_{PS}. In addition, it would be interesting to compare bromination of PS brushes on flat substrates with that on convex substrate. To this end, the curvature of the convex substrate may help to alleviate confinement effects acting on the grafted macromolecules. Experiments are currently in progress to address those points.

Acknowledgment. This work was supported by the National Science Foundation under Contracts DMR-0353102 and OISE-0730243. The authors gratefully acknowledge Hanna Gracz for performing the NMR experiments.

References and Notes

(1) Alsheh, D.; Marom, G. *J. Appl. Polym. Sci.* **1978**, *22*, 3177–3184.
(2) Prins, M.; Marom, G.; Levy, M. *J. Appl. Polym. Sci.* **1976**, *20*, 2971–2978.
(3) Brauman, S. K. *J. Fire Retard. Chem.* **1980**, *7*, 130–135.
(4) British Patent 1,569,070, Nov 6, **1980**.
(5) Zhao, W.; Zhao, X.; Rafailovich, M. H.; Sokolov, J.; Mansfield, T.; Stein, R. S.; Composto, R. C.; Kramer, E. J.; Jones, R. A. L.; Sansone, M.; Nelson, M. *Physica B* **1991**, *173*, 43–46.
(6) Genzer, J.; Faldi, A.; Oslanec, R.; Composto, R. J. *Macromolecules* **1996**, *29*, 5438–5445.
(7) Faldi, A.; Genzer, J.; Composto, R. J.; Dozier, W. D. *Phys. Rev. Lett.* **1995**, *74*, 3388–3391.
(8) Genzer, J.; Composto, R. J. *Europhys. Lett.* **1997**, *38*, 171–176.
(9) Genzer, J.; Composto, R. J. *Macromolecules* **1998**, *31*, 870–878.
(10) Strobl, G. R.; Bendler, J. T.; Kambour, R. P.; Shultz, A. R. *Macromolecules* **1986**, *19*, 2683–2689.
(11) Bruder, F.; Brenn, R. *Macromolecules* **1991**, *24*, 5552–5557.
(12) Bucknall, D. G. *Prog. Mater. Sci.* **2004**, *49*, 713–786.
(13) Benkoski, J. J.; Fredrickson, G. H.; Kramer, E. J. *J. Polym. Sci., Part B: Polym. Phys.* **2001**, *39*, 2363–2377.
(14) Kulasekere, R.; Kaiser, H.; Anker, J. F.; Russell, T. P.; Brown, H. R.; Hawker, C. J.; Mayes, A. M. *Macromolecules* **1996**, *29*, 5493–5496.
(15) Pellegrini, N. N.; Sikka, M.; Satija, S. K.; Winey, K. I. *Polymer* **2000**, *41*, 2701–2704.
(16) Mansky, P.; Liu, Y.; Huang, E.; Russell, T. P.; Hawker, C. *Science* **1997**, *275*, 1458–1460.
(17) Takashima, K.; Tanaka, G.; Yamakawa, H. *Polym. J.* **1971**, *2*, 245–256.
(18) Noguchi, Y.; Aoki, A.; Tanaka, G.; Yamakawa, H. *J. Chem. Phys.* **1970**, *52*, 2651–2657.
(19) Ham, G. E. *J. Polym. Sci., Part C: Polym. Symp.* **1976**, *56*, 305–309.
(20) Heublein, G.; Wondraczek, R. *Makromol. Chem.* **1977**, *178*, 1853–1867.
(21) Konigsberg, I.; Jagurgrodzinski, J. *J. Polym. Sci., Part A: Polym. Chem.* **1983**, *21*, 2535−2546, 2649−2663.
(22) Yoshida, E. *J. Polym. Sci., Part A: Polym. Chem.* **1996**, *34*, 2937–2943.
(23) Farrall, M. J.; Frechet, J. M. J. *J. Org. Chem.* **1976**, *41*, 3877–3882.
(24) Guibert, Y.; Brossas, J. *Polym. Bull.* **1979**, *1*, 293.
(25) Kambour, R. P.; Bendler, J. T.; Bopp, R. C. *Macromolecules* **1983**, *16*, 753–757.
(26) Kambour, R. P.; Bendler, J. T. *Macromolecules* **1986**, *19*, 2679–2682.
(27) Camps, M.; Montheard, J. P.; Benrokia, F. *Eur. Polym. J.* **1991**, *27*, 389–396.
(28) Bielski, R.; Fréchet, J. M. J.; Fusco, J. V.; Powers, K. W.; Wang, H. C. *J. Polym. Sci., Part A: Polym. Chem.* **1993**, *31*, 755–762.
(29) Fréchet, J. M. J.; Bielski, R.; Wang, H. C.; Fusco, J. V.; Powers, K. W. *Rubber Chem. Technol.* **1993**, *66*, 98–108.
(30) Andrews, L. J.; Keefer, R. M. *J. Am. Chem. Soc.* **1956**, *78*, 4549–4553.
(31) Yates, K.; Wright, W. V. *Can. J. Chem.* **1967**, *45*, 167–173.
(32) Caille, S. Y.; Corriu, R. J. P. *Tetrahedron* **1969**, *25*, 2005–2022.
(33) Camps, M.; Montheard, J. P.; Benrokia, F.; Camps, J. M.; Pham, Q. T. *Eur. Polym. J.* **1990**, *26* (1), 53–59.
(34) Cancelier, J. P. *Bull. Soc. Chim. Fr.* **1971**, *5*, 1785–1788.
(35) Brown, H. C.; Nelson, K. L. *J. Am. Chem. Soc.* **1953**, *75*, 6292–6299.
(36) Clark, J. H. In *Chemistry of Waste Minimization*; Chapman & Hall: London, 1995.

(37) Epstein, D. M.; Meyerstein, D. *Inorg. Chem. Commun.* **2001**, *4*, 705–707.
(38) Narender, N.; Mohan, K. V. V. K.; Reddy, R. V.; Srinivasu, P.; Kulkarni, S. J.; Raghavan, K. V. *J. Mol. Catal. A* **2003**, *192*, 73–77.
(39) Khanarian, G.; Cais, R. E.; Kometani, J. M.; Tonelli, A. E. *Macromolecules* **1982**, *15*, 866–869.
(40) Semler, J. J.; Jhon, Y. K.; Tonelli, A.; Beevers, M.; Krishnamoorti, R.; Genzer, J. *Adv. Mater.* **2007**, *19*, 2877–2883.
(41) Orofino, T. A.; Mickey, J. W. *J. Chem. Phys.* **1963**, *38*, 2512–2520.
(42) Orofino, T. A.; Ciferri, A. *J. Phys. Chem.* **1964**, *68*, 3136–3141.
(43) Mays, J. W.; Hadjichristidis, N.; Fetters, L. J. *Macromolecules* **1985**, *18*, 2231–2236.
(44) Jhon, Y. K.; Krishnamoorti, R.; Genzer, J. Manuscript in preparation.
(45) Strickland, L. A.; Hall, C. K.; Genzer, J. Manuscript submitted for publication.
(46) Santiso, E. E.; George, A. M.; Gubbins, K. E.; Buongiorno Nardelli, M. *J. Chem. Phys.* **2006**, *125*, 084711.
(47) Santiso, E. E.; Kostov, M. K.; George, A. M.; Buongiorno Nardelli, M.; Gubbins, K. E. *Appl. Surf. Sci.* **2007**, *253*, 5570–5579.
(48) Halls, M. D.; Schlegel, H. B. *J. Phys. Chem. B* **2002**, *106*, 1921–1925.
(49) Turner, C. H.; Gubbins, K. E. *J. Chem. Phys.* **2003**, *119*, 6057–6067.
(50) Byl, O.; Kondratyuk, P.; Yates, J. T. *J. Phys. Chem. B* **2003**, *107*, 4277–4279.
(51) Kaneko, K.; Fukuzaki, N.; Kakei, K.; Suzuki, T.; Ozeki, S. *Langmuir* **1989**, *5*, 960–965.
(52) Imai, J.; Souma, M.; Ozeki, S.; Suzuki, T.; Kaneko, K. *J. Phys. Chem.* **1991**, *95*, 9955–9960.
(53) Matyjaszewski, K.; Miller, P. J.; Shukla, N.; Immaraporn, B.; Gelman, A.; Luokala, B. B.; Siclovan, T. M.; Kickelbick, G.; Vallant, T.; Hoffmann, H.; Pakula, T. *Macromolecules* **1999**, *32*, 8716–8724.
(54) Gorman, C. B.; Petrie, R. J.; Genzer, J. *Macromolecules*, in press.
(55) Nédez, C.; Ray, J.-L. *Langmuir* **1999**, *15*, 5932–5936.
(56) Ando, T.; Kato, M.; Kamigaito, M.; Sawamoto, M. *Macromolecules* **1996**, *29*, 1070–1072.
(57) Matyjaszewski, K.; Patten, T. E.; Xia, J. *J. Am. Chem. Soc.* **1997**, *119*, 674–680.
(58) Boyes, S. G.; Brittain, W. J.; Weng, X.; Cheng, S. Z. D. *Macromolecules* **2002**, *35*, 4960–4967.
(59) Brandrup, J.; Immergut, E. H.; Grulke, E. A. In *Polymer Handbook*, 4th ed.; Wiley-Interscience: New York, 1999.
(60) Tompkins, H. G.; Irene, E. A. In *Handbook of Ellipsometry*; William Andrew Publishing: New York, 2005.
(61) Han, J.; Semler, J. J.; Jhon, Y. K.; Ryu, C. Y.; Genzer, J. Manuscript in preparation.
(62) Jhon, Y. K.; Cheong, I. W.; Kim, J. H. *Colloids Surf., A* **2001**, *179*, 71–78.
(63) Socrates, G. In *Infrared Characteristic Group Frequencies; Tables and Charts*; John Wiley & Sons: New York, 1994.
(64) Khokhlov, A. R.; Khalatur, P. G. *Physica A* **1998**, *249*, 253–261.
(65) Khokhlov, A. R.; Khalatur, P. G. *Phys. Rev. Lett.* **1999**, *82*, 3456–3459.
(66) Neyens, A. H.; Jungers, J. C. *Bull. Soc. Chim. Fr.* **1959**, *10*, 1481–1491.
(67) Rouquier, A.; Sajus, L.; Jungers, J. C. *Bull. Soc. Chim. Fr.* **1963**, *2*, 217–223.
(68) Buckles, R. E.; Hausman, E. A.; Wheeler, N. G. *J. Am. Chem. Soc.* **1950**, *76*, 2494–2496.
(69) Smith, K. *J. Chem. Tech. Biotechnol.* **1997**, *68*, 432–436.
(70) McKillop, A.; Bromley, D. *Tetrahedron Lett.* **1969**, *21*, 1623–1626.
(71) McGary, C. W.; Okamoto, Y.; Brown, H. C. *J. Am. Chem. Soc.* **1955**, *77*, 3037–3043.
(72) Brown, H. C.; Wirkkala, R. A. *J. Am. Chem. Soc.* **1966**, *88*, 1447–1452.
(73) Rothbaum, H. P.; Ting, I.; Robertson, P. W. *J. Chem. Soc.* **1948**, 980–984.
(74) Robertson, P. W. *J. Chem. Soc.* **1954**, 1267–1270.
(75) De la Mare, P. B. D.; Robertson, P. W. *J. Chem. Soc.* **1943**, 279–281.
(76) Keefer, R. M.; Andrews, L. J. *J. Am. Chem. Soc.* **1950**, *72*, 4677–4681.
(77) Keefer, R. M.; Ottenberg, A.; Andrews, L. J. *J. Am. Chem. Soc.* **1956**, *78*, 255–259.
(78) Niclaes, H.; Jungers, J. C. *Bull. Soc. Chim. Fr.* **1962**, *3*, 582.
(79) Persoons, A.; Jungers, J. C. *Bull. Soc. Chim. Fr.* **1968**, *7*, 2729.
(80) Berthelot, J.; Guette, C.; Desbene, P.; Basselier, J.; Chaquin, P.; Masure, D. *Can. J. Chem.* **1990**, *68*, 464–470.
(81) Dubois, J. E.; Aaron, J. J.; Alcais, P.; Doucet, J. P.; Rothenberg, F.; Uzan, R. *J. Am. Chem. Soc.* **1972**, *94*, 6823–6828.
(82) Tomlinson, M. R.; Genzer, J. *Macromolecules* **2003**, *36*, 3449–3451.
(83) Tomlinson, M. R.; Genzer, J. *Langmuir* **2005**, *21*, 11552–11555.
(84) Strickland, L. A.; Hall, C. K.; Genzer, J. Manuscript in preparation.
(85) Jhon, Y. K.; Shin, K. W.; Genzer, J. Manuscript in preparation.

MA8011653